



A Shake-Table Test Investigating the Drift Capacity of Reinforced Masonry Wall Systems

Jianyu Cheng¹, Andreas Koutras², and P. Benson Shing³

ABSTRACT

An accurate quantification of the displacement capacity of a reinforced masonry shear-wall system is of critical importance to seismic design because it has a direct implication on the seismic force modification factor, which is the R factor in ASCE 7. In spite of the shear capacity design requirement in TMS 402, special reinforced masonry walls within a building system could still develop shear-dominated behavior, which is perceived to be far more brittle than flexural behavior. These walls have a low shear-span ratio either because of the wall geometry (i.e., a low height-to-length ratio) or the coupling forces introduced by the horizontal diaphragms, which are often ignored in design. Although shear-dominated walls appeared to be very brittle in quasi-static tests conducted on single planar wall segments, reinforced masonry structures survived major ground shaking well in past earthquakes. This could be partly attributed to the beneficial influence of wall flanges as well as the over-strength of the system. Flanged walls are common in masonry buildings, but their behavior is not well understood because of the lack of laboratory test data. Furthermore, other walls or columns that are present in the structural system to carry gravity loads could enhance the lateral resistance of the shear walls and the displacement capacity of the system by providing axial restraints as well as alternative load paths for gravity loads. A research project is being carried out with shake-table tests to investigate the displacement capacity of shear-dominated reinforced masonry wall systems. This paper presents results of the first shake-table test conducted in this project on a full-scale single-story coupled T-wall system. The structure was tested to a drift ratio exceeding 15% without collapse.

KEYWORDS: reinforced masonry, walls, displacement, seismic, shear, earthquake

¹ Graduate Student Researcher; University of California, San Diego; La Jolla, CA, USA; j7cheng@eng.ucsd.edu

² Graduate Student Researcher; University of California, San Diego; La Jolla, CA, USA; akoutras@eng.ucsd.edu

³ Professor; University of California, San Diego; La Jolla, CA, USA; pshing@ucsd.edu

INTRODUCTION

An accurate quantification of the displacement capacity or ductility of a reinforced masonry shear-wall system is of critical importance to seismic design because it has a direct implication on the seismic force modification factor, namely, the R factor in ASCE /SEI 7-10 (ASCE/SEI 2010). The value of the R factor for special reinforced masonry wall systems is based on the expectation that these wall systems can develop a certain amount of ductility in a severe seismic event. However, in spite of the shear capacity design requirement in TMS 402 (TMS 2016), a special reinforced masonry wall system could develop shear-dominated behavior when a wall system has wall elements with low shear-span ratios, which might or might not be anticipated in the design. For example, strong coupling forces that could be introduced by horizontal diaphragms could reduce the shear-span ratio of a wall but are often ignored in design. The behavior and lateral resistance of shear-dominated reinforced masonry walls have been studied by many researchers. For example, Voon and Ingham (2006), Shing et al. (1991), and Ahmadi (2012) conducted quasi-static tests on shear-dominated single wall segments. They showed that walls with shear-dominated behavior were significantly more brittle than flexure-dominated walls. In spite of this, reinforced masonry structures performed well in past earthquake events, surviving strong ground shaking without collapse. This could be attributed to the beneficial influence of wall flanges. Flanged walls are common in masonry buildings, but their behavior is not well understood because of the lack of laboratory data. Furthermore, other walls or columns that are present in the structural system to carry gravity loads could enhance the lateral resistance of the shear walls and the displacement capacity of the system by providing axial restraints as well as alternative load paths for gravity loads.

Mavros et al. (2016), Stavridis et al. (2016), and Koutras and Shing (2017) conducted shake-table tests to study the seismic performance of reinforced masonry wall systems with shear-dominated wall components. The two-story fully grouted reinforced masonry wall system tested by Mavros et al. (2016) had only 20% strength degradation when the 1st story reached a drift ratio of 2%. Similar observations were obtained in the other two studies. This is in contrast to the behavior of shear-dominated rectangular single wall segments tested by Voon and Ingham (2006), Shing et al. (1991), and Ahmadi (2012), which exhibited severe load degradations at drift ratios way less than 1%. The more ductile behavior observed in the wall systems in these shake-table tests can be attributed to the factors mentioned above. However, the influence of these factors is not well quantified, but is important to investigate in order to have an accurate assessment of the collapse potential of a reinforced masonry wall system, which is an essential consideration for seismic design.

This paper presents the findings of a current research project supported by the National Science Foundation (NSF) to investigate the displacement capacity of shear-dominated reinforced masonry wall systems. As part of this study, two fully grouted reinforced masonry wall systems are to be tested on a shake table to collapse or the verge of collapse. The designs of the two specimens and results of the tests conducted on the first specimen are presented in this paper.

SPECIMEN DESIGN

Figure 1 shows the layouts of the two reinforced masonry shear wall systems, Specimen 1 and Specimen 2, designed to be tested on the uniaxial outdoor shake table at the University of California San Diego. Each specimen has two T-walls as the seismic force resisting elements. Specimen 2 has six additional rectangular walls oriented perpendicular to the direction of the shake-table motion. They are referred to as the out-of-

plane walls. These two specimens are intended to investigate the influence of the out-of-plane walls on the seismic resistance of a wall system.

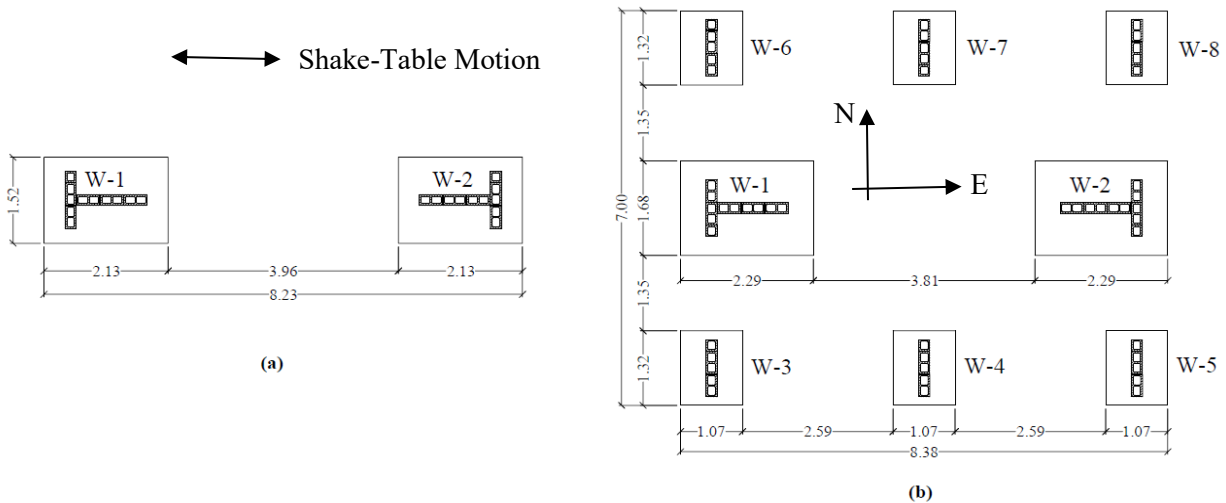


Figure 1. Plan view of footing and wall layout (dimension in meters): (a) Specimen 1; (b) Specimen 2

The flanged walls in both specimens have the same dimensions and reinforcement arrangement. The reinforcing bars are Grade 60. As shown in Figure 2, each T-wall has six No. 4 (129 mm²) bars spaced at 8 inches (20 cm) on center in the web, and three No. 4 (129 mm²) bars spaced at 16 inches (41 cm) in the flange for the vertical reinforcement. The horizontal bars in the web and the flange are No. 3's (71 mm²) spaced at 16 inches (41 cm) on center. This corresponds to a vertical reinforcement ratio of 0.0030 and a horizontal reinforcement ratio of 0.0009. Each of the rectangular walls perpendicular to the direction of shaking in Specimen 2 has No. 4 (129 mm²) bars for the vertical reinforcement, and No. 3 (71 mm²) bars for the horizontal reinforcement, both spaced at 16 inches (41 cm) on center. The reinforcement ratios comply with the prescriptive requirements of TMS 402 (TMS 2016) for special walls, but the spacing of the reinforcing bars in the flanges of the T-walls slightly violates the maximum spacing requirement. The vertical reinforcement ran continuously from the walls into the footings without lap-splices, and each bar ended with a 90-degree standard hook in the footing conforming to ACI 318 provisions (ACI 318-08). The surface of the concrete footing underneath each wall was intentionally roughened to increase the frictional resistance.

The roof weights of Specimens 1 and 2 are 55.1 kips (245 kN) and 135 kips (601 kN), respectively. They were so determined that the wall systems can reach their ultimate seismic load capacities with a moderately scaled ground motion that is within the capacity of the shake table. The roof weight of Specimen 1 was so selected that its T-walls have the same axial compressive load ratio as the T-walls in Specimen 2. Since Specimen 1 had the same T-wall design as Specimen 2 but a different seismic mass, the input ground motions for Specimen 1 had to be scaled with a similitude law so that the structure would experience the same seismic load demands as Specimen 2. Since the roof slab is very stiff, the tributary roof load, P , on each wall was assumed to be proportional to the wall's axial stiffness (which is proportional to the wall's cross-sectional area). The axial compressive load ratio, $P/f'_m A_g$, for each T-wall was calculated to be 0.016, where A_g is the cross-sectional area of the wall. The compressive strength of masonry, f'_m , was specified to be 2.5 ksi (17 MPa). As shown in Figure 2, the roof slab for Specimen 1 consisted of 10-in-thick (25 cm)

precast prestressed hollow-core planks with a 5-inch-thick cast-in-place concrete topping. Two reinforced concrete blocks, each with a size of 10 ft × 10 ft × 14 in (3.0 m × 3.0 m × 36 cm) were secured on top of the roof slab to achieve the intended roof mass. For Specimen 2, the roof slab consists of 8-inch-thick (20 cm) hollow-core planks with a 3-inch (7.6 cm) concrete topping. It has four additional concrete slabs for added mass. The size of each concrete slab for Specimen 2 is 16.5 ft × 10 ft × 10 in (5.0 m × 3.0 m × 25 cm).

The diagonal shear, flexural, and shear sliding strengths of the T-walls were checked to ensure that they would develop diagonal shear-dominated behavior. The diagonal shear strength was calculated with the formula in Chapter 9 of TMS 402 (TMS 2016). The flexural strength was calculated using an axial force – moment interaction diagram based on the recommendations in TMS 402, assuming a fixed-fixed end condition due to the high stiffness of the roof diaphragms. The shear sliding resistance was calculated by the shear friction formula provided in Chapter 9 of TMS 402. The calculated diagonal shear, flexural and shear sliding strengths of each T-wall are 73 kips (326 kN), 80 kips (355 kN), and 89 kips (397 kN), respectively, based on the masonry compressive strength of 2.5 ksi (17 MPa), and the expected yield strength of 68 ksi (469 MPa) for the reinforcing bars.

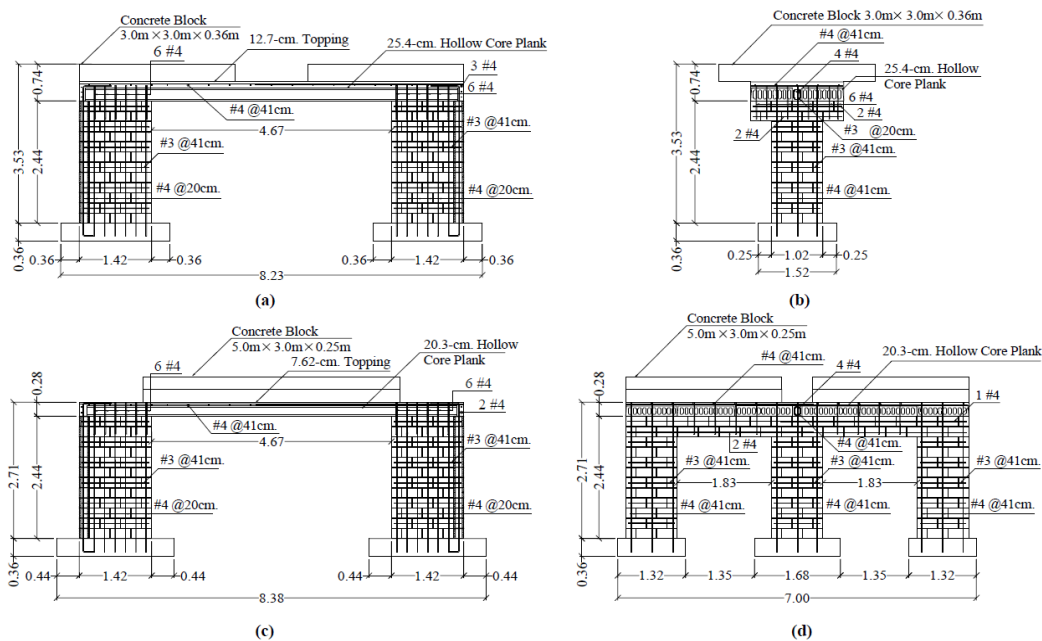


Figure 2. Reinforcement details (dimension in meters): (a) South elevation view of Specimen 1; (b) West elevation view of Specimen 1; (c) South elevation view of Specimen 2; (d) West elevation view of Specimen 2

INSTRUMENTATION FOR SPECIMEN 1

The instrumentation for Specimen 1 included 76 strain gages, 8 tri-axial accelerometers, and 56 displacement transducers to measure the rebar strains, roof and footing accelerations, and displacements at different locations. Strain gages were installed on the vertical bars near the top and bottom of each wall to measure potential yielding due to the flexure of the wall. The remaining strain gages were installed both on vertical and horizontal bars at locations where potential diagonal cracks could pass. The locations of the strain gages will be shown later in Figure 8 together with the yielding observed. As shown in Figure 3, four tri-axial

accelerometers were installed at the corners of the roof slab to measure the roof acceleration during the tests. The other 4 accelerometers were installed on the top of the concrete footings. Figure 3 also shows the locations where the string and linear potentiometers were mounted. The string potentiometers were used to measure the shear deformation of each wall and the vertical displacement of the roof slab. The relative horizontal displacement between the roof and the table (the story drift) was measured by two string potentiometers mounted on an aluminum frame installed on a stiff braced HSS column, which was fixed on the table. The linear potentiometers were used to measure the relative vertical displacements along the two sides of each wall (to obtain data to calculate wall curvature along the wall height), sliding between the concrete footings and the reinforced masonry walls, sliding between the walls and the roof slab, and any sliding between the web and the flange of each T-wall.

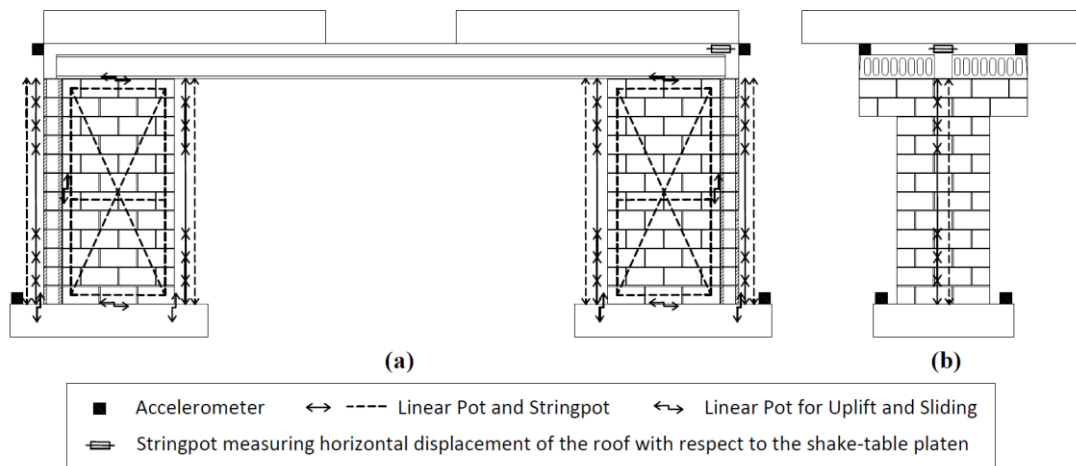


Figure 3. Locations of accelerometers and displacement transducers in Specimen 1: (a) South elevation view; (b) West elevation view

TEST SETUP AND TEST SEQUENCE FOR SPECIMEN 1

The test setup for Specimen 1 is shown in Figure 4. As shown, the flanged wall on the west side of the shake table is identified as Wall 1, while the wall on the east side is identified as Wall 2. Testing was conducted in two phases. In the first phase, the structure was subjected to earthquake ground motions, reaching a roof drift ratio of 2.53% with a significant load degradation. In the second phase, testing was continued by subjecting the already damaged structure to quasi-static lateral loading until the lateral resistance dropped close to zero.

As shown in Figure 4, four safety concrete pedestals were secured on the shake table as a catch system to prevent damage to the table in case the specimen collapsed. A clearance of 10 inches (25 cm) was provided between the top surface of the pedestals and the bottom surface of the roof slab.

In Phase 1, the structure was subjected to a sequence of 7 earthquake motions that had been derived by scaling the acceleration of the Mulholland station record from the 1994 Northridge Earthquake. The motions were applied in 4 different intensities, with the amplitudes scaled to 45%, 90%, 120%, and 133% of the original earthquake record, respectively. After each motion, the specimen was subjected to a white-noise excitation to identify any change in its natural period. The white noise had a root-mean-square amplitude of 0.03g and a duration of 3 minutes. Since Specimens 1 and 2 had different seismic weights (sum

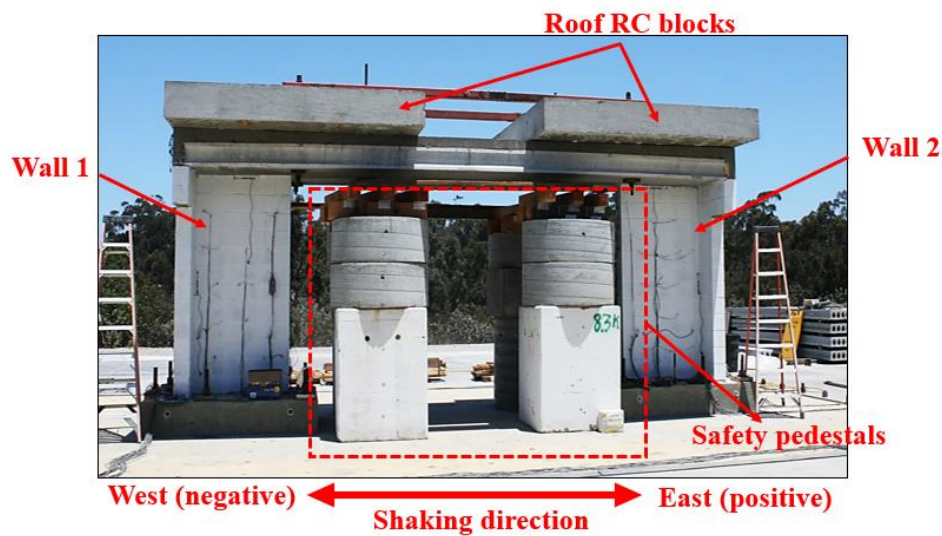


Figure 4. Test setup for Specimen 1

of the total roof weight and the masonry weight above the mid-height of the shear walls), additional scaling was applied to the time and amplitude of the earthquake records used for Specimen 1 to attain the dynamic similitude between the two structures. The ground acceleration was scaled up by a factor of 2.4 (seismic weight of Specimen 2 / seismic weight of Specimen 1), and the time was compressed by a factor of $\sqrt{1/s_a} = 0.65$, with the assumption that both structures have the same lateral stiffness and strength. Figure 5 shows the acceleration spectra of the original earthquake record at the four intensity levels and the acceleration time history scaled to 133% of the original intensity, all after the similitude scaling was applied.

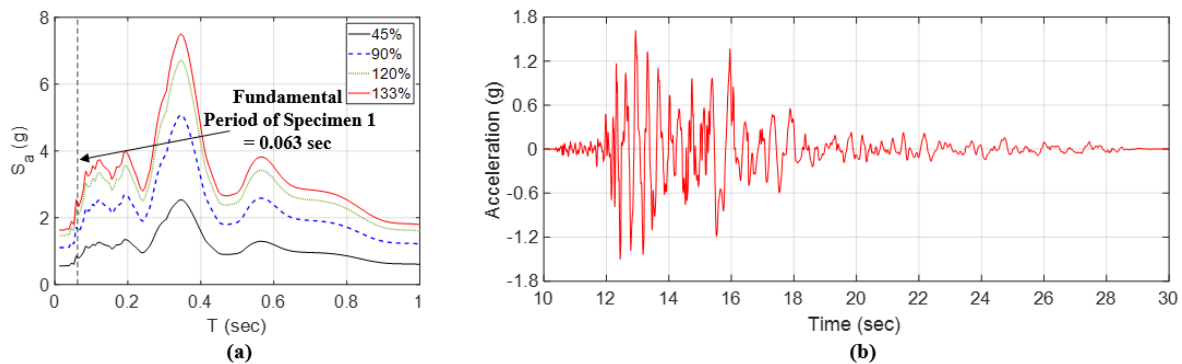


Figure 5. Ground motions used in the shake-table tests for Specimen 1: (a) Acceleration spectra of the Northridge record at 4 different intensities; (b) ground acceleration time history of the Northridge record scaled to 133% of the original intensity

In Phase 2, the structure was subjected to a quasi-static lateral load with the test setup shown in Figure 6. Two cables were used to pull the roof slab by moving the table away from a stiff steel reaction tower, to which the other ends of the cables were attached. The load was monitored with two load cells. The horizontal roof displacement was increased until the lateral resistance of the tested structure dropped close to zero.

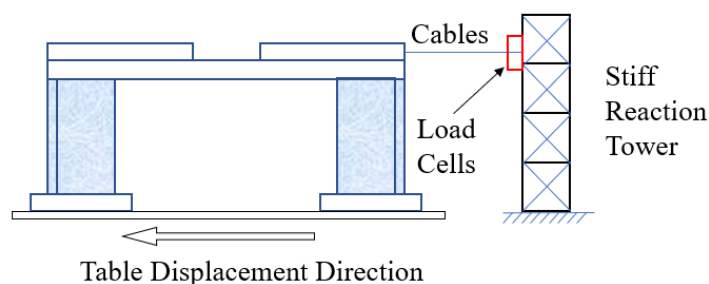


Figure 6. Quasi-static test setup for Specimen 1

TEST RESULTS AND OBSERVATIONS FOR SPECIMEN 1

Dynamic Tests with 45% and 90% Northridge Motions

Two low-intensity and three mid-intensity tests were conducted by scaling the Northridge record to 45% and 90%, respectively. The two low-intensity motions and the first mid-intensity motion were to check the instrumentation. No visible cracks were observed on the wall surface during the two 45% level motions. Figure 7 shows that the fundamental period of the intact specimen (0.063 second) had not changed after these shakings.

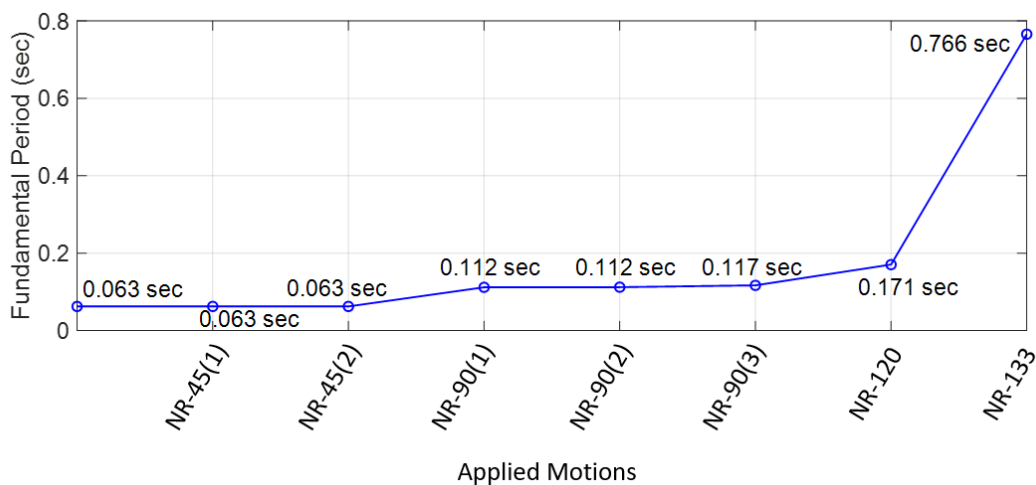


Figure 7. Change of fundamental period of Specimen 1

After the first shaking with the 90% level motion, the fundamental period of the specimen increased by 0.05 second, indicating that some damage had occurred during the test. For both walls, the vertical bars at two extreme sides had yielded in tension near the wall base, as shown in Figure 8. After three shakings with the 90% level motions, it was observed that a few flexural cracks initiated in the webs near the bottom of the two walls. As shown in Figure 7, the fundamental period measured from the white-noise tests increased by 0.005 second. All the vertical bars in the flanges had yielded at the first masonry course from the base. Moreover, both walls had one vertical bar in the flange yielded at the second course from the base, indicating an extension of the plastic zones.

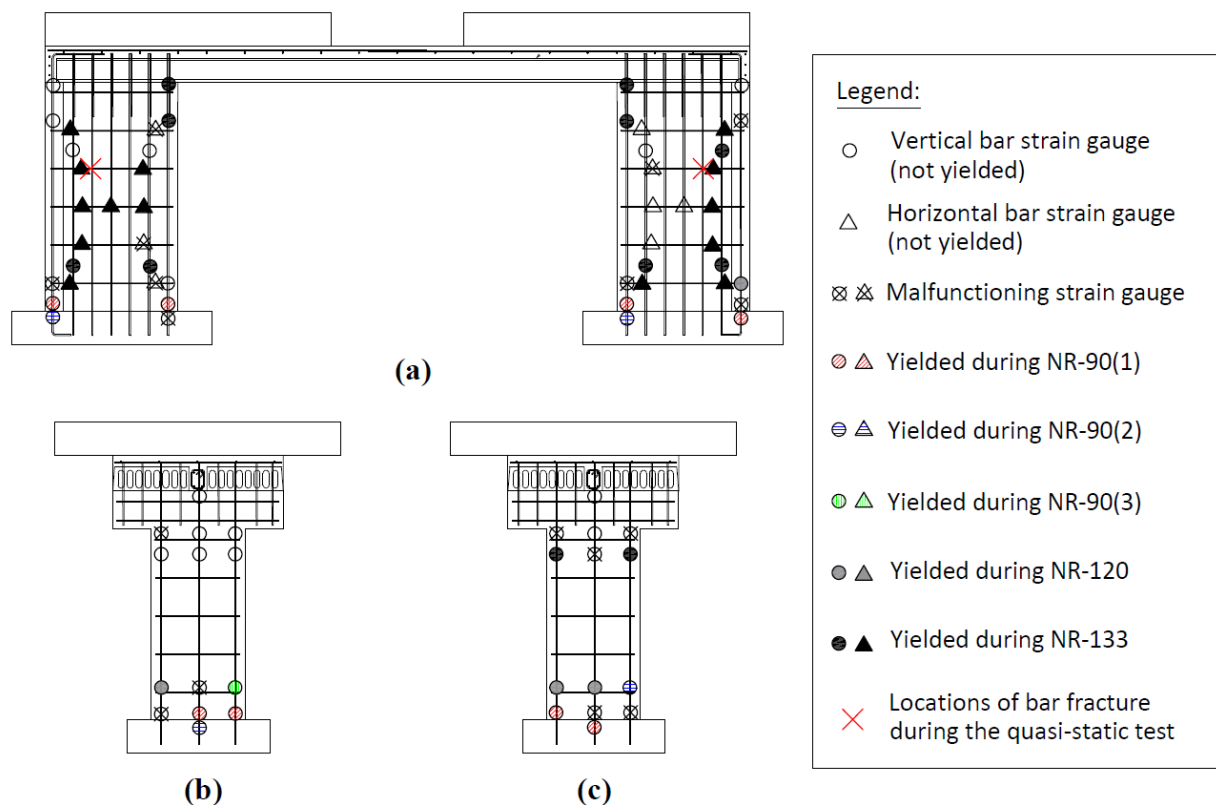


Figure 8. Yielding of reinforcing bars in Specimen 1: (a) Webs of two flanged walls; (b) Flange of Wall 1; (c) Flange of Wall 2

Dynamic Test with 120% Northridge Motion

A test was performed with a 120% level motion. During this test, horizontal flexural cracks propagated in the webs and flanges near the bottom of both walls. Figure 9 shows the base shear - vs. - roof drift hysteresis curves obtained for the structure during this motion. The base shear was evaluated from the average roof acceleration along the shaking direction, measured by the four accelerometers installed on the roof slab, and the seismic mass that consisted of the total roof mass and the masonry mass above the mid-height of the walls. During this motion, the maximum resistance developed by the structure reached 132 kips (588 kN) at a roof drift ratio of 0.35% (based on the wall height of 2.44 m and the roof horizontal displacement of 8.64 mm). As shown in Figure 7, the fundamental period of the specimen increased from 0.117 to 0.171 second, which was largely attributed to the development of flexural cracks and the yielding of the rebars. The strain gage measurements show that the extreme bar near the free edge of each wall web had yielded in tension at the second masonry course from the wall base. All the vertical bars in the flanges of both walls had also yielded at the second course from the base, as shown in Figure 8.

Dynamic Test with 133% Northridge Motion

The last dynamic test was conducted with a 133% level motion. In this test, the walls developed shear failure. The specimen exhibited significant lateral drifts due to the resonance effect experienced by the structure as it softened. Damage suffered in this test shifted the fundamental period of the structure from 0.171 to 0.766 second, as shown in Figure 7, while the predominant period of the ground motion is around 0.35 second as shown in Figure 5. Figure 10 shows that severe diagonal shear cracks developed on the webs

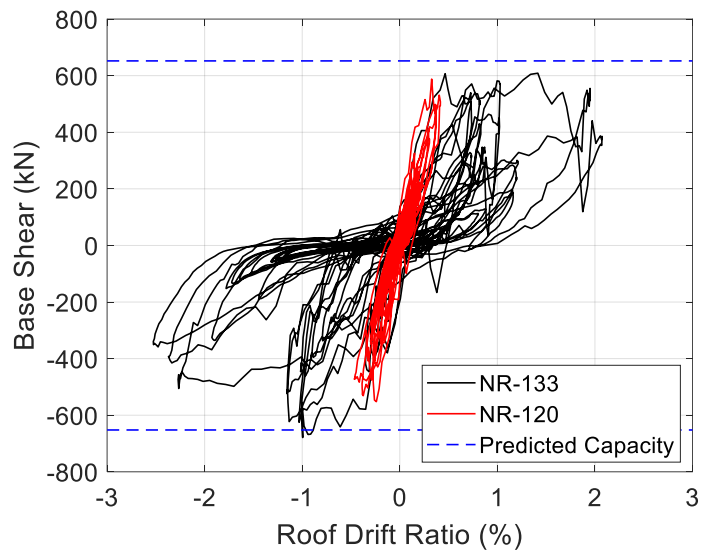


Figure 9. Base shear-vs.- roof drift ratio hysteresis curves from the last two shake-table tests

of both walls, accompanied by the spalling of masonry along the major diagonal cracks. However, none of the diagonal cracks had propagated into the flanges. Wall 2 showed base crushing and buckling of the extreme vertical bar in the web near the wall base. Figure 8 shows that most of the vertical and horizontal bars yielded at the locations where the major diagonal cracks developed. Some of the vertical bars also yielded near the top of the walls.

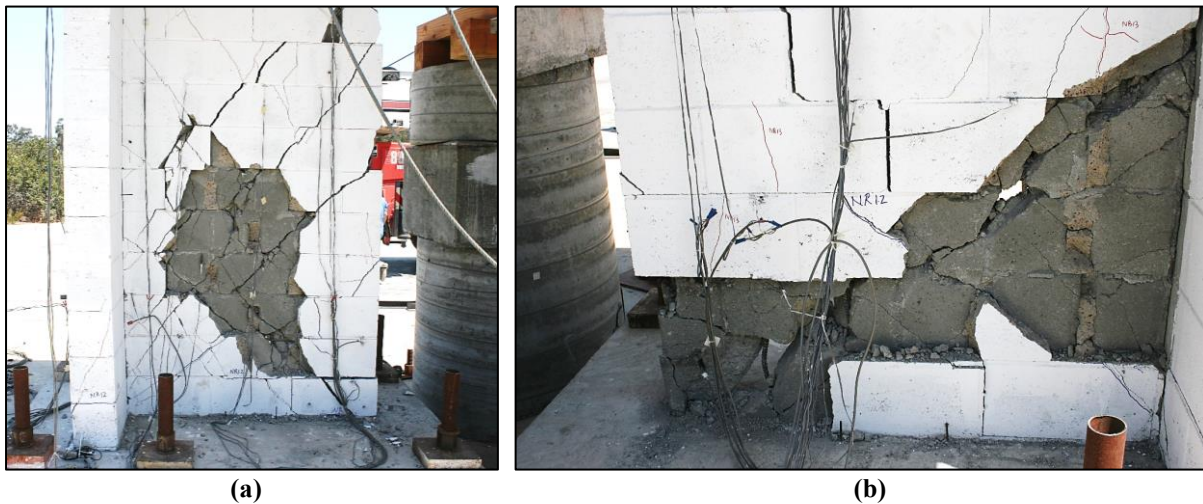


Figure 10. Damage after the test with 133% Northridge motion: (a) Wall 1 (b) Wall 2

The base shear-vs.-roof drift hysteresis curve for the structure (Figure 9) shows that a peak strength of 152 kips (679 kN) was reached at a roof drift ratio of about 1% in the negative (west) direction. The peak strength of the specimen is close to the shear strength of 154 kips (685 kN) calculated with the formula given in TMS 402 (TMS 2016). The masonry compressive strength and the yield strength of the horizontal reinforcing bars used in the strength calculation were the average strengths obtained from the masonry prism tests and tension tests of the bars. They are 2.93 ksi (20.2 MPa) and 63.0 ksi (434 MPa), respectively.

A maximum roof drift ratio of 2.53% was reached in the west direction. At this drift level, the lateral resistance of the tested structure dropped to 76.3 kips (340 kN), which was about 50% of the peak strength.

Quasi-Static Pull Test

During the quasi-static pull test, the diagonal cracks in each wall continued to extend and open as the horizontal roof displacement increased. Severe crushing and spalling of the masonry was observed. As shown in Figure 11, a roof drift ratio of 16.7% (42.4-cm roof horizontal displacement) was reached when the lateral resistance of the wall system dropped to 9.9 kips (44 kN), which is 6% of the peak strength. Horizontal cracks were observed in the wall flanges, and a few diagonal cracks in the webs had extended into the flanges (Figure 12). At the roof drift level of 16.7%, only the flanges were supporting the roof slab to prevent it from collapse as most of the masonry in the web had spalled off. There was no contact between the safety pedestals and the roof slab as the vertical displacement of the roof slab was negligible. During the quasi-static test, two horizontal bars in the webs (one in each wall) fractured, as shown in Figure 8. For both walls, fracture occurred in the fourth horizontal bar from the base, at locations close to the flanges.

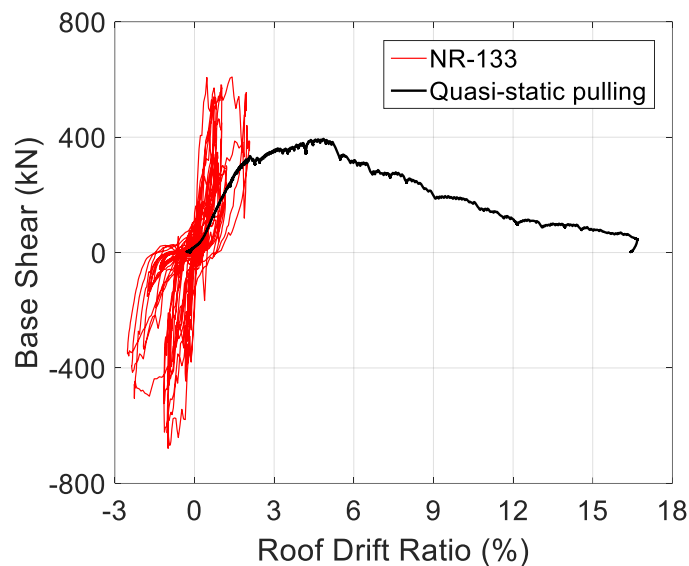


Figure 11. Base shear- vs.-roof drift ratio curves from the dynamic test with the 133% Northridge motion and the quasi-static test



Figure 12. Specimen 1 after the static pull test

SUMMARY AND CONCLUSIONS

This paper presents a study to investigate the displacement capacity of shear-dominated reinforced masonry wall systems. Two specimens, each having two T-walls as the seismic load resisting system, were designed and to be tested on a shake table. In the design, the roof slabs were assumed to be rigid, and the walls were so reinforced that the failure mechanism was expected to be dominated by shear. However, in practice, the moment restraints imposed by floor and roof diaphragms are often ignored, which may result in a design with significant flexural overstrength and likely dominated by a shear mechanism as the test specimens considered here. Specimen 1 was tested on a shake table with earthquake motions as well as a quasi-static pull force. The walls exhibited flexural behavior during the 90% and 120% Northridge motions, but had failures eventually dominated by diagonal shear cracks during the 133% Northridge motion. The maximum lateral resistance developed by Specimen 1 is close to the shear strength calculated with the formula in TMS 402 (TMS 2016). A maximum drift ratio of 16.7% was reached in the quasi-static test, at which the lateral resistance of the wall system dropped to 6% of the peak strength. This drift capacity is significantly higher than what was observed in quasi-static wall tests conducted in the past on single wall segments. The large displacement capacity observed here can be largely attributed to the wall flanges, which continued to carry the vertical load when the webs were severely damaged. Comparing to Specimen 1, Specimen 2 has six additional out-of-plane rectangular walls, which may further improve the performance of the wall system. Specimen 2 will be tested in early 2019. The test results will help to calibrate and validate analytical models to obtain a more accurate assessment of the collapse potential of reinforced masonry wall systems, which is an important consideration for seismic design.

ACKNOWLEDGMENTS

This project is supported with funding from the National Science Foundation (NSF) under Award No. CMMI-1728685. The support of the NHERI program of the NSF for the shake-table tests conducted at the UC San Diego NHERI facility is also gratefully acknowledged. The authors are most grateful to RCP Block and Brick for their generous donation of the concrete masonry units for the construction of the test specimens, and to the technical staff of the Powell Structural Engineering Laboratories and the Englekirk Structural Engineering Center, in which the shake-table facility is located, for their support in the experimental work. The authors would also like to thank Jeffrey Lee and Joyner Deamer, undergraduate students in the REU program, for their assistance in test preparation. However, opinions expressed in this paper are those of the authors and do not necessarily reflect those of the sponsor.

REFERENCES

- ACI Committee, & International Organization for Standardization. (2008). *Building code requirements for structural concrete (ACI 318-08) and commentary*. American Concrete Institute.
- Ahmadi, F. (2012). "Displacement-based Seismic Design and Tools for Reinforced Masonry Shear-Wall Structures," *Ph.D. Dissertation*, Department of Civil Engineering, University of Texas at Austin, Austin, TX.
- ASCE (2010). *Minimum Design Loads for Buildings and Other Structures*, ASCE/SEI Standard 7-10.

Koutras, A., and Shing, P. B. (2017). "Shake-Table Testing and Performance Assessment of a Partially Grouted Reinforced Masonry Building," *International Conference on Experimental Vibration Analysis for Civil Engineering Structures* (pp. 480-493). Springer, Cham.

Mavros, M., F. Ahmadi, P. B. Shing, R. E. Klingner, D. McLean, and A. Stavridis. (2016). "Shake-table tests of a full-scale two-story shear-dominated reinforced masonry wall structure," *Journal of Structural Engineering* 142, no. 10: 04016078.

Shing, P. B., Noland, J. L., Spaeh, H. P., Klamerus, E. W., and Schuller, M. P. (1991). "Response of Single-Story Reinforced Masonry Shear Walls to In-Plane Lateral Loads," *Report No. 3.1(a)-2*, US-Japan Coordinated Program for Masonry Building Research, University of Colorado at Boulder, Boulder, CO.

Stavridis, A., Ahmadi, F., Mavros, M., Shing, P. B., Klingner, R. E., and McLean, D. (2016). "Shake-table tests of a full-scale three-story reinforced masonry shear wall structure." *Journal of Structural Engineering* 142, no. 10: 04016074.

TMS 402/602 (2013, 2016). *Building code requirements for masonry structures*, The Masonry Society (TMS), Longmont, CO.

Voon, K. C. and Ingham, J. M. (2006). "Experimental In-Plane Shear Strength Investigation of Reinforced Concrete Masonry Walls," *Journal of Structural Engineering*, 132(3), 400-408.